Physica Scripta. Vol. 72, 265–273, 2005

Phase Transition Property of Ferroelectric Superlattice with three Alternative Layers from Ising Model in a Transverse Field

A. Tabyaoui[a,c], A. Ainane[a,b,c,*], M. Saber[a,b,c] and I. Lukyanchuk[c]

[a]Physics Department, Faculty of Sciences, University of Moulay Ismail, B.P. 4010, Meknes, Morocco
[b]Max Planck Institut für Physik Komplexer Systeme, Nöthnitzer Str. 38, D-01187, Dresden, Germany
[c]Laboratoire de Physique de la Matière Condensée, Département de Physique, Faculté des Sciences, Université Picardie, F-80039 Amiens Cedex, France

Received December 8, 2004; revised version received February 17, 2005; accepted March 1, 2005

PACS numbers: 75.70.−i, 75.70.Ak, 75.70.Cn

Abstract

The critical temperature, polarization and dielecric susceptibility in ferroelectric superlattices with three alternative layers described by a transverse spin−1/2 Ising model are studied using the effective field theory with a probability distribution technique. We discuss an L layer superlattice of simple cubic symmetry with nearest-neighbor interactions. We derive the phase diagram, the polarization profiles and the dielectric susceptibilities. In such superlattices, the critical temperature can shift to either lower or higher temperature compared with the corresponding bulk value. The superlattice dielectric longitudinal susceptibility diverges at the superlattice critical temperature.

1. Introduction

Artificially fabricated superlattices have been studied in great detail in semiconducting materials. The physical properties, which differ dramatically from simple solids in this new class of materials, have aroused great interest in the synthesis and study of superlattices in other materials. In layered ferromagnetic materials, it has been found experimentally that one can obtain a rich variety of magnetic behaviour depending of the materials, the thickness and number of slabs and of the applied field [1–2]. Theoretical works devoted to the magnetic and phase transition properties of superlattices formed from alternating layers of different materials have been carried out [3–4]. In ferroelectric materials, the fabrication of heterostructures has been possible only in recent years owing to advanced film deposition techniques. Monoatomic layer growth of $(BaTiO_3)/(SrTiO_3)$ with perovskite-type structure was achived by Iijima *et al*. [4].

It is believed that the formation of ferroelectric superlattices is not only a new field of material science but will also provide new opportunities for ferroelectric materials applications and throw light on the understanding of the mechanism giving rise to ferroelectricity. Many experiments show that the interfacial coupling may have nontrivial effects on the dielectric properties of ferroelectric thin films, such as the enhancement of the dielectric constant [5–6]. The dielectric properties of the ferroelectric superlattice depend sensitively on the interfacial coupling and the thickness of the components [7–9]. Theoretically, the static and dynamic properties of ferroelectric superlattices have been studied by Tilley [10] and Schwenk *et al.* [11–13] on the basis of the Ginzburg-Landau phenomenological theory. Qu *et al.* [14] discussed the dependence of the Curie temperature on the strength of interface coupling and layer thickness using a pseudospin theory based on the Ising model in a transverse field. The physical properties such as the longitudinal polarization and dielectric susceptibility were discussed using the same model in mean field approximation [15]. Despite the simplicity of the transverse Ising model, it was successful in describing the phase transition behavior of ferroelectrics [16] by modifying the exchange coupling and the transverse field at the surface. Wang *et al*. [17–18], and Saber *et al.* [19] successfully extended the transverse Ising model to the study of surface and size effects in ferroelectrics, such as ferroelectric superlattice [8] and [20]. Recently Wang *et al*. [21] studied a ferroelectric superlattice with three alternative layers using the transverse Ising model in the mean field approximation. Also ferroelectric superlattice with three alternative layers has been fabricated successfully by high-pressure pulsed laser deposition method very recently [22].

Our aim in this paper is to study the polarizations and the dielectric susceptibilities of a transverse spin-1/2 Ising superlattice within the framework of the effective field theory [23]. This technique is believed to give more exact results than those of the standard mean-field approximation. In section 2 we give the equations that determine the polarizations and the critical temperature of the superlattice as functions of temperature, exchange interactions, transverse field and slabs thicknesses. In section 3, we discuss the phase transition behavior of the dielectric longitudinal susceptibility as well as the spontaneous polarization of ferroelectric superlattices and a brief conclusion is given in section 4. Our results are in good agreement with those obtained recently by C. L. Wang *et al.* [21] using the mean field approximation.

2. Formalism

The pseudospin theory based on the transverse Ising model is generally believed to be a good microscopic description of bulk properties of hydrogen-bonded ferroelectric systems of KH_2PO_4 type. It has also been applied successfully to many other systems [11, 12] and in the study of surface effects on the static and dynamic properties of semi-infinite ferroelectric [13] and ferroelectric thin films [14–15] and [17]. Let us consider a superlattice consisting of three different ferroelectric materials A, B and C with a simple cubic structure. The periodic condition suggests that we only have to consider one unit cell which interacts via its nearest-neighbors via interface couplings. The situation is depicted in Fig. 1 which shows clearly the interaction strength between any nearest-neighboring spins and also the strength of the transverse field at any site. The corresponding number of layers in A, B and C is L_a, L_b and L_c and the thickness of the cell is $L = L_a + L_b + L_c + 3$. The Hamiltonian of the system is given by

$$H = -\sum_{\langle ij \rangle} J_{ij}\ \sigma_{iz}\sigma_{jz} - \Omega \sum_{i} \sigma_{ix} \tag{1}$$

*Corresponding author: ainane@fsmek.ac.ma

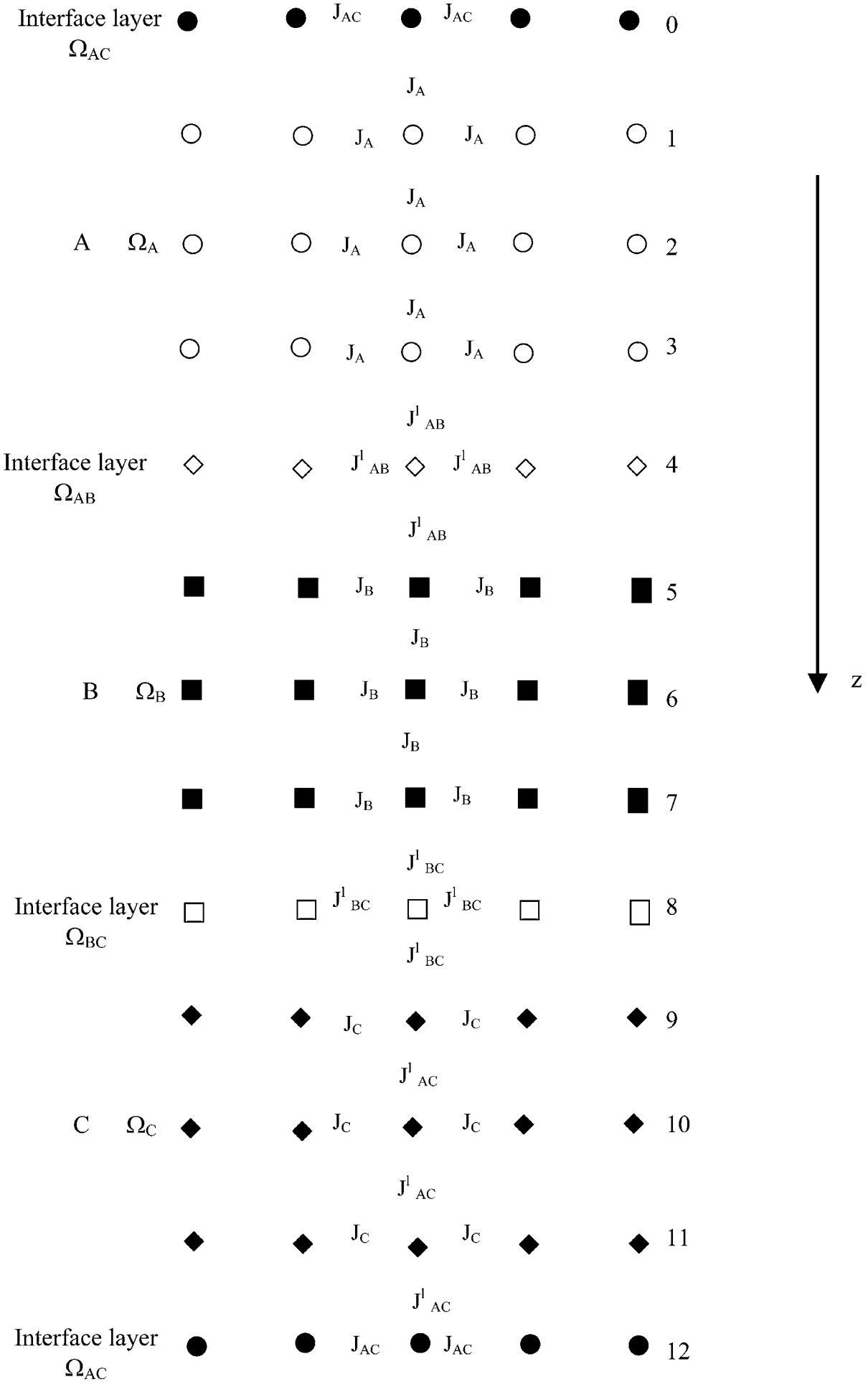

Fig. 1. One period of a three alternative ferroelectric superlattice $A_3/B_3/C_3$. The z direction is normal to the interfaces.

where σ_{iz} and σ_{ix} denote the z and x components of a quantum spin $\vec{\sigma}_i$ of magnitude $\sigma = 1/2$ at site i, J_{ij} is the strength of the exchange interaction between the spins at nearest-neighbor sites i and j, Ω is the transverse field which for an H-bond ferroelectric represents the proton tunneling between equilibrium positions on the H bonds. Using the effective field theory with a probabilty distribution technique [23], the layer longitudinal and transverse polarizations of the superlattice are derived in the same manner as in [24] and they are given by

$$m_{n\alpha} = \langle \sigma_{n\alpha} \rangle = \left\langle f_\alpha \left(\sum_j J_{ij}\sigma_{jz}, \Omega \right) \right\rangle \tag{2}$$

where $\alpha = z$ and x for the longitudinal and transverse polarizations respectively and

$$f_z \left(\sum_j J_{ij}\sigma_{jz}, \Omega \right) = \frac{1}{2} \frac{\sum_j J_{ij}\sigma_{jz}}{[(\sum_j J_{ij}\sigma_{jz})^2 + \Omega^2)]^{\frac{1}{2}}} \times \tanh \left\{ \tfrac{1}{2}\beta \left[\left(\sum_j J_{ij}\sigma_{jz} \right)^2 + \Omega^2 \right]^{\frac{1}{2}} \right\}, \tag{3}$$

$$f_x \left(\sum_j J_{ij}\sigma_{jz}, \Omega \right) = f_z \left(\Omega, \sum_j J_{ij}\sigma_{jz} \right) \tag{4}$$

$\beta = \frac{1}{k_B T}$ (we take $k_B = 1$ for simplicity) and T is the temperature. In Eq. (2), $\langle \cdots \rangle$ indicates the usual canonical ensemble thermal average for a given configuration and the sum runs over all nearest-neighbors of the spin $\vec{\sigma}_i$.

To perform thermal averaging on the right hand side of Eq. (2), we follow the general approach described in Ref. [23]. First of all, in the spirit of the effective field theory, multispin-correlation functions are approximated by products of single spin averages. We then take advantage of the integral representation of the Dirac delta distribution, in order to write Eq. (2) in the following form

$$m_{n\alpha} = \int \mathrm{d}\omega f_\alpha(\omega, \Omega) \frac{1}{2\pi} \int \left[\mathrm{d}t \exp(\mathrm{i}wt) \prod_j \langle \exp(\mathrm{i}tJ_{ij}\sigma_{jz}) \rangle \right]. \tag{5}$$

We now introduce the probability distribution of the spin variables (for details see Ref. [23])

$$P(\sigma_{nz}) = \tfrac{1}{2}[(1 - 2m_{nz})\delta(\sigma_{nz} + \tfrac{1}{2}) + (1 + 2m_{nz})\delta(\sigma_{nz} - \tfrac{1}{2})]. \tag{6}$$

Using this expression and Eq. (5), we get the following equations for the layer polarizations

$$m_{n\alpha} = 2^{-N-2N_0} \sum_{\mu=0}^{N} \sum_{\mu_1=0}^{N_0} \sum_{\mu_2=0}^{N_0} \{C_\mu^N C_{\mu_1}^{N_0} C_{\mu_2}^{N_0} (1 - 2m_{nz})^\mu \times (1 + 2m_{nz})^{N-\mu} (1 - 2m_{n-1,z})^{\mu_1} (1 + 2m_{n-1,z})^{N_0-\mu_1} \times (1 - 2m_{n+1,z})^{\mu_2} (1 + 2m_{n+1,z})^{N_0-\mu_2} \ f_\alpha(y_n, \Omega)\} \tag{7}$$

where

$$y_n = \tfrac{1}{2}[J_{nn}(N - 2\mu) + J_{n,n-1}(N_0 - 2\mu_1) + J_{n,n+1}(N_0 - 2\mu_2)]. \tag{8}$$

In this equation (7), N and N_0 denote respectively the coordination numbers on the parallel planes and inter-planes and for the case of a simple cubic lattice which is considered here, one has $N = 4$ and $N_0 = 1$ and C_k^l are the binomial coefficients, $C_k^l = \frac{l!}{k!(l-k)!}$. The longitudinal and transverse polarizations of the superlattice are defined by

$$m_\alpha = \frac{1}{L} \sum_{n=1}^{L} m_{n\alpha}. \tag{9}$$

We have thus obtained the self-consistent equations (7) for the layer longitudinal and transverse polarizations m_{nz} and m_{nx} that can be solved directly by numerical iteration. As we are interested in the calculation of the longitudinal ordering near the transition critical temperature, the usual argument that the layer longitudinal polarization m_{nz} tends to zero as the temperature approaches its critical value, allows us to consider only terms linear in m_{nz} because higher order terms tend to zero faster than m_{nz} on approaching a critical temperature. Consequently, all terms of order higher than linear terms in Eqs. (7) can be neglected. This leads to the set of simultaneous equations

$$m_{nz} = A_{n,n-1}m_{n-1,z} + A_{n,n}m_{nz} + A_{n,n+1}m_{n+1,z} \tag{10}$$

which can be written as

$$M\,\vec{m_z} = 0 \tag{11}$$

where $\vec{m}_z$ is a vector of components $(m_{1z}, \ldots, m_{nz}, \ldots, m_{Lz})$ and M is a matrix of elements

$$M_{i,j} = (A_{i,i} - 1)\delta_{i,j} + A_{i,j}(\delta_{i,\,j-1} + \delta_{i,\,j+1}). \tag{12}$$

The only non zero elements of the matrix M are given by

$$M_{n,n-1} = 2^{-N-2N_0} \sum_{\mu=0}^{N} \sum_{\mu_1=0}^{N_0} \sum_{\mu_2=0}^{N_0} \sum_{i=0}^{\mu_1} \sum_{j=0}^{N_0-\mu_1} [(-1)^i 2^{i+j} \delta_{1,i+j} \times C_\mu^N C_{\mu_1}^{N_0} C_{\mu_2}^{N_0} C_i^{\mu_1} C_j^{N_0-\mu_1} f_z(y_n, \Omega)], \tag{13}$$

$$M_{n,n} = 2^{-N-2N_0} \sum_{\mu=0}^{N} \sum_{\mu_1=0}^{N_0} \sum_{\mu_2=0}^{N_0} \sum_{i=0}^{\mu} \sum_{j=0}^{N_0-\mu} [(-1)^i 2^{i+j} \delta_{1,i+j} \times C_\mu^N C_{\mu_1}^{N_0} C_{\mu_2}^{N_0} C_i^{\mu} C_j^{N-\mu} f_z(y_n, \Omega)] - 1, \tag{14}$$

$$M_{n,n+1} = 2^{-N-2N_0} \sum_{\mu=0}^{N} \sum_{\mu_1=0}^{N_0} \sum_{\mu_2=0}^{N_0} \sum_{i=0}^{\mu_2} \sum_{j=0}^{N_0-\mu_2} [(-1)^i 2^{i+j} \delta_{1,i+j} \times C_\mu^N C_{\mu_1}^{N_0} C_{\mu_2}^{N_0} C_i^{\mu_2} C_j^{N_0-\mu_2} f_z(y_n, \Omega)], \tag{15}$$

with the periodic boundary conditions $M_{1,0} = M_{1,L}$ and $M_{L,L+1} = M_{L,1}$. All the information about the critical temperature of the system is contained in Eq. (11). Up to now we did not assign precise values of the exchange interactions and the strength of the transverse field and unit cell width: the terms in matrix (11) are general ones.

In a general case, for arbitrary exchange interactions, transverse field and unit cell width, the evaluation of the critical temperature relies on numerical solution of the system of linear Eqs. (11). These equations can be satisfied by nonzero polarization vectors $\vec{m_z}$ only if

$$\det M = 0. \tag{16}$$

In general, Eq. (16) can be satisfied for $L = L_a + L_b + L_c + 3$ different values of the critical temperature T_c from which we choose the one corresponding to the highest possible transition

temperature (see discussion in Ref. [25]). This value of T_c corresponds to a solution having $m_{1z}, m_{2z}, \ldots m_{Lz}$ positive, which is compatible with a ferromagnetic longitudinal ordering. The other formal solutions correspond in principle to other types of ordering that usually do not occur here (Ferchmin and Maciejewski [25]).

3. Results and discussion

The dielectric properties are important in practice and in particular the dielectric longitudinal susceptibilities are interesting physical quantities which describe the characteristics of the change of the polarizations with the fields and can show the phase transitions properties, particularly its critical temperature. The phase transition is usually predicted by the abnormal behavior of the dielectric longitudinal susceptibility at the critical temperature. In order to obtain the dielectric longitudinal susceptibility, we apply a uniform longitudinal magnetic field h across the superlattice, which adds to the Hamiltonian Eq. (1) a term

$$H_1 = -h \sum_{i=1}^{L} \sigma_{iz} \tag{17}$$

describing the interaction of the longitudinal polarization with the magnetic field h. In order to calculate the dielectric longitudinal susceptibility, we apply the formalism of section 2. Eqs. (7) continue to apply but the parameter y now is replaced by $y + h$. The dielectric longitudinal susceptibility of the n^{th} layer is given by

$$\chi_{nz} = \frac{\partial m_{nz}}{\partial h}\Big)_{h=0}. \tag{18}$$

The details of the calculus of the layer dielectric longitudinal susceptibilities are given in appendix I. To evaluate the dieletric longitudinal susceptibility of the superlattice, we follow the formalism of Wang *et al.* [26]. As each layer can be treated as a capacitor, the capacitance of the superlattice is the sum of the capacitances of each of the layers connected in series. The total reciprocal permittivity is the sum of the reciprocal permittivities at each of the layers. Thus the total dielectric susceptibility (the dielectric longitudinal susceptibility of the superlattice) χ_z is determined from

$$(1 + \chi_z)^{-1} = \frac{1}{L} \sum_{n=1}^{L} (1 + \chi_{nz})^{-1} \tag{19}$$

where L is the total number of layers.

We obtain the layer longitudinal and transverse polarizations from Eqs. (7) and the longitudinal and transverse polarization of the superlattice from Eq. (9). The layer dieletric longitudinal susceptibility and the dieletric longitudinal susceptibility of the superlattice can be obtained respectively from Eqs. (18) and (19).

We have calculated many curves of the temperature dependencies of the layer polarizations and dielectric susceptibilities for different values of the above parameters. We take throughout this paper the same values used by Wang *et al.* [21], $J_{aa} = 15$, $J_{bb} = 7$, $J_{cc} = 2$, and $\Omega_{aa} = 20$, $\Omega_{bb} = 10$, $\Omega_{cc} = 1$, which mean the Curie temperature of bulk material A is higher than that of bulk material B. For the interface layers, the parameters are taken as $\Omega_{lm} = (\Omega_l + \Omega_m)/2$ and $J_{lm} = \sqrt{J_l . J_m}$ where $l, m = A, B, C$. We also include the anisotropy in lateral and longitudinal direction by assuming that the interaction coefficient between two sites in the same layer, J_{ij} is different from that between two sites in two adjacent layers, J^l_{ij}. For simplicity, in the calculation and without loss of generality, we take $J^l_{ij}/J_{ij} = 1.5$.

The period dependence of the Curie temperature is shown in Fig. 2, where T_{cm} is the Curie temperature of superlattice

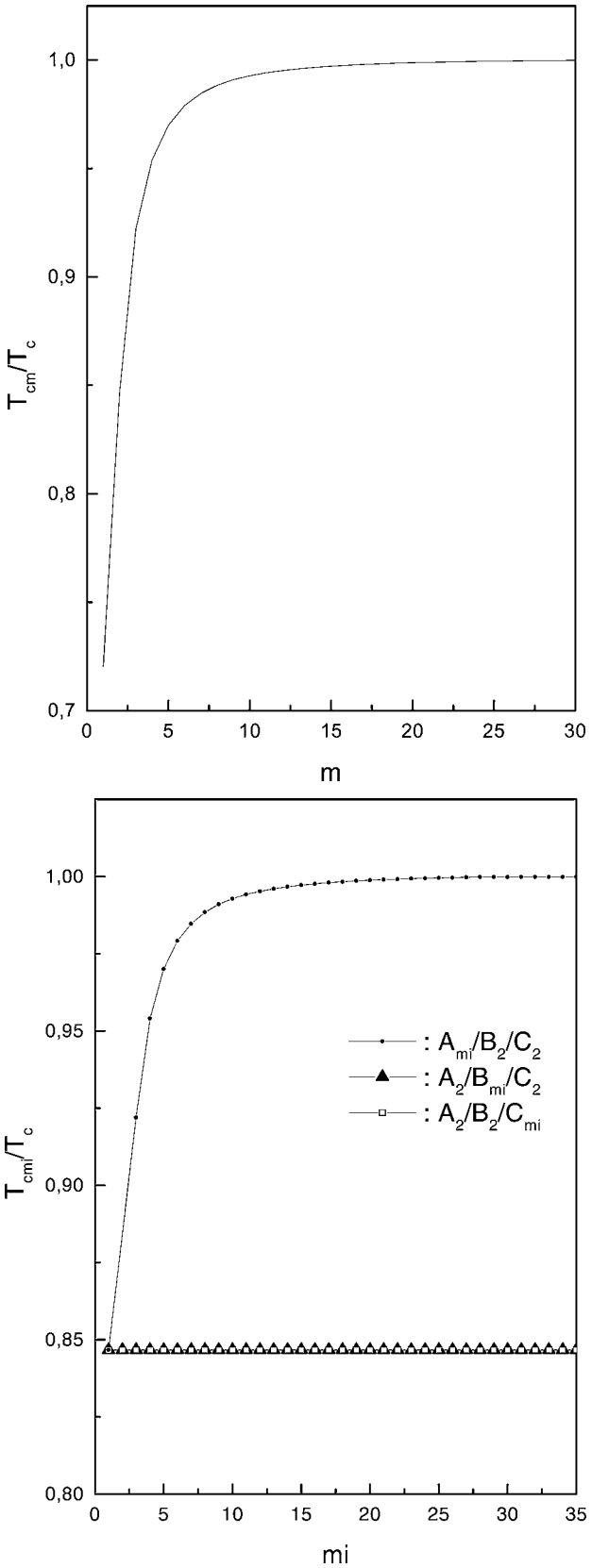

Fig. 2. a: The period dependence of the Curie temperature of the superlattice $A_m/B_m/C_m$. T_{cm} is the Curie temperature of the superlattice, T_c is that of bulk material A. b: The period dependence of the Curie temperature of $A_{mi}/B_2/C_2$, $A_2/B_{mi}/C_2$ and $A_2/B_2/C_{mi}$ superlattices. T_{cmi} is the Curie temperature of the superlattices $A_{mi}/B_2/C_2$, $A_2/B_{mi}/C_2$ and $A_2/B_2/C_{mi}$, T_c is that of bulk material A.

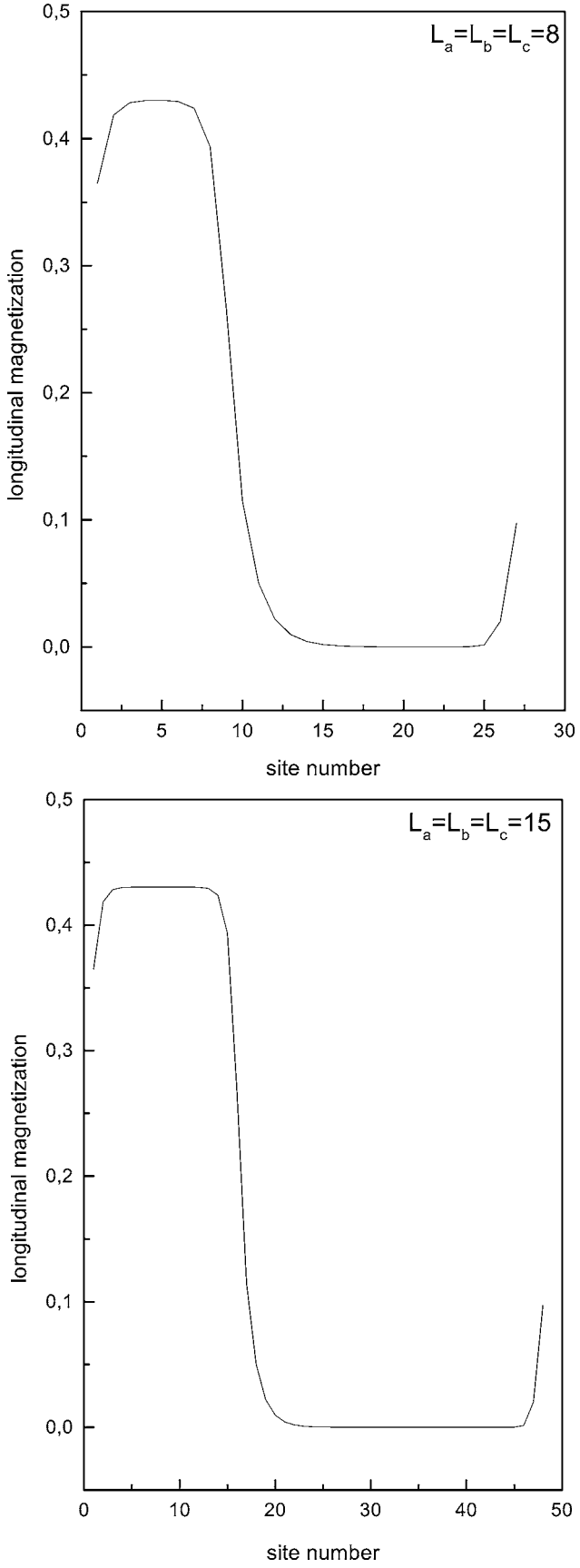

Fig. 3. a: The profiles of the longitudinal polarization at a temperature of $0.4T_c$ when $L_a = L_b = L_c = 8$. b: The profiles of the longitudinal polarization at a temperature of $0.4T_c$ when $L_a = L_b = L_c = 30$.

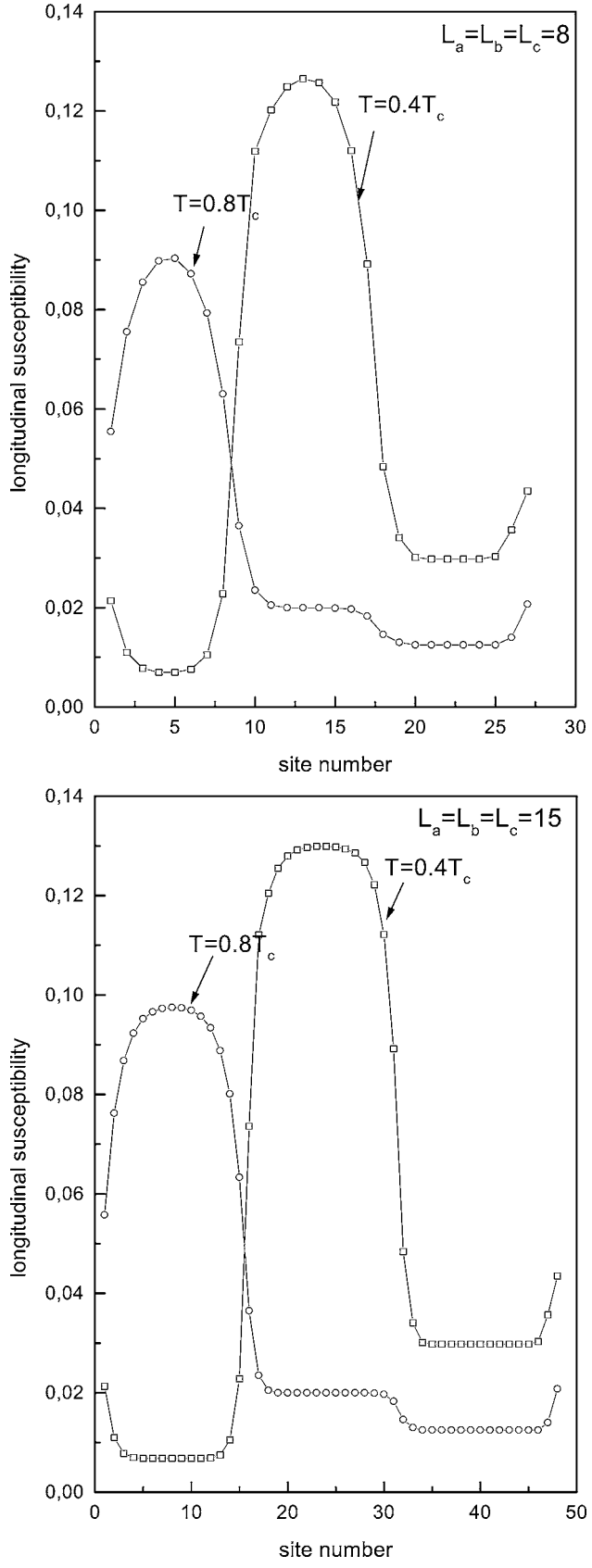

Fig. 4. a: The profiles of the dielectric longitudinal susceptibility at temperatures of $0.4T_c$ and $0.8T_c$ when $L_a = L_b = L_c = 8$. b: The profiles of the dieletric longitudinal susceptibility at temperatures of $0.4T_c$ and $0.8T_c$ of $A_{15}/B_{15}/C_{15}$ superlattice.

$A_m/B_m/C_m$, T_c is the Curie temperature of bulk material A, and T_{cmi} is that of superlattice $A_{mi}/B_2/C_2$ or $A_2/B_{mi}/C_2$ or $A_2/B_2/C_{mi}$. Fig. 2a shows the Curie temperature of the superlattice with the same layer thickness for A-layers, B-layers and C-layers. From this figure, we can see that the Curie temperature drops very quickly at the small period side. The Curie temperature of the superlattice approaches the Curie temperature of bulk material A when the period increases. Fig. 2b

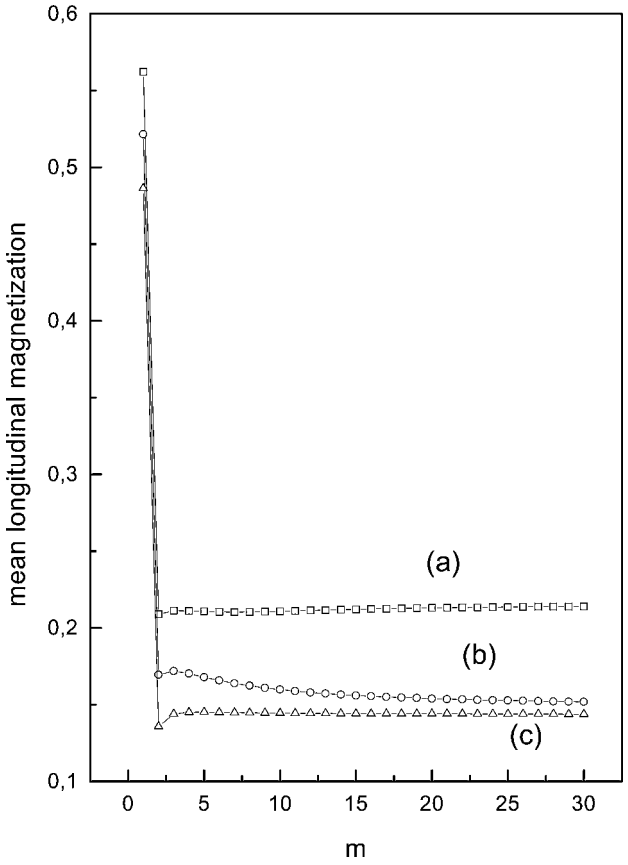

Fig. 5. The period dependence of the mean longitudinal polarization of $A_m/B_m/C_m$ superlattice at different temperatures, curve (a) $T = 0.3T_c$, (b) $T = 0.35T_c$, (c) $T = 0.4T_c$.

shows the Curie temperature varation with the layer thickness of one material. It is obvious that the layer thickness of A-layers has a dominant influence on the Curie temperature of the superlattice, while the thickness of B-layers and C-layers have almost no effect on it. Such a result is easy to understand, since bulk material A has a higher Curie temperature than bulk materials B and C.

Fig. 3 shows the profiles of the polarization within one period of the superlattice at a temperature of $0.4T_c$. Fig. 3a is for a superlattice with relative short period of 27 layers, Fig. 3b is for a superlattice with relative long period of 48 layers. The polarization shows step-like distribution between A-layers and B-layers, as well as B-layers and C-layers. The step-like feature becomes more distinct when the period of the superlattice increases. The profiles of the dielectric susceptibility at $0.4T_c$ and $0.8T_c$ are shown in Fig. 4. At $T = 0.4T_c$, the B-layers are ferroelectric. At $T = 0.8T_c$, they are paraelectric. In both cases, the interface layer between B and C and its around layers have higher dielectric susceptibility value than that of the other layers. From Figs. 3 and 4 we can see that the behavior of the interface layer between B-layers and C-layers as well as its around layers look like a site-driven phase transition.

The period dependences of the mean polarization and the mean dielectric susceptibility at different temperatures are shown in Figs. 5 and 6 respectively. The mean polarization shows a minimum and the mean dielectric susceptibility shows a maximum around the small period range. This is similar to polarization and dielectric susceptibility of a superlattice with two alternative layers [20]. The minimum of polarization becomes less obvious when the temperature increases. When the temperature is the same, the period at which the polarization minimizes is the same as that at which the dielectric susceptibility maximizes. As is shown in Fig. 6a, when the temperature approaches T_c^B, the peak

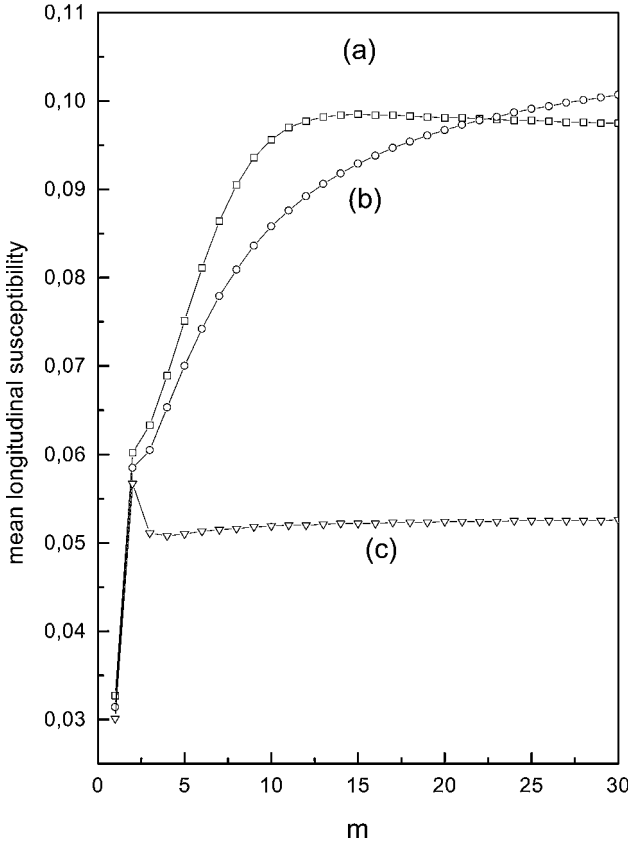

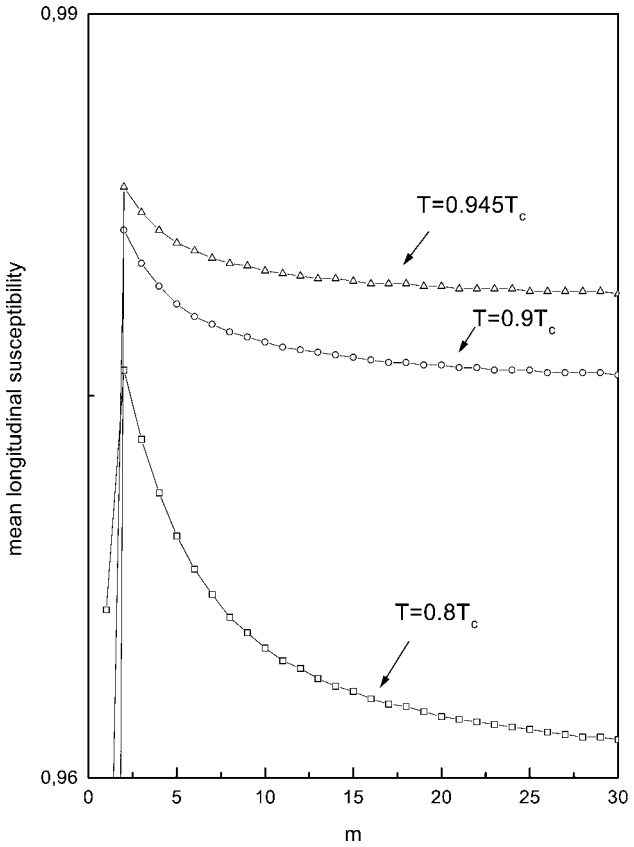

Fig. 6. a: The period dependence of the mean dielectric longitudinal susceptibility of $A_m/B_m/C_m$ superlattice below T_c^B. T_c^B is the Curie temperature of bulk material B. b: The period dependence of the mean dielectric longitudinal susceptibility of $A_m/B_m/C_m$ superlattice above T_c^B. T_c^B is the Curie temperature of bulk material B.

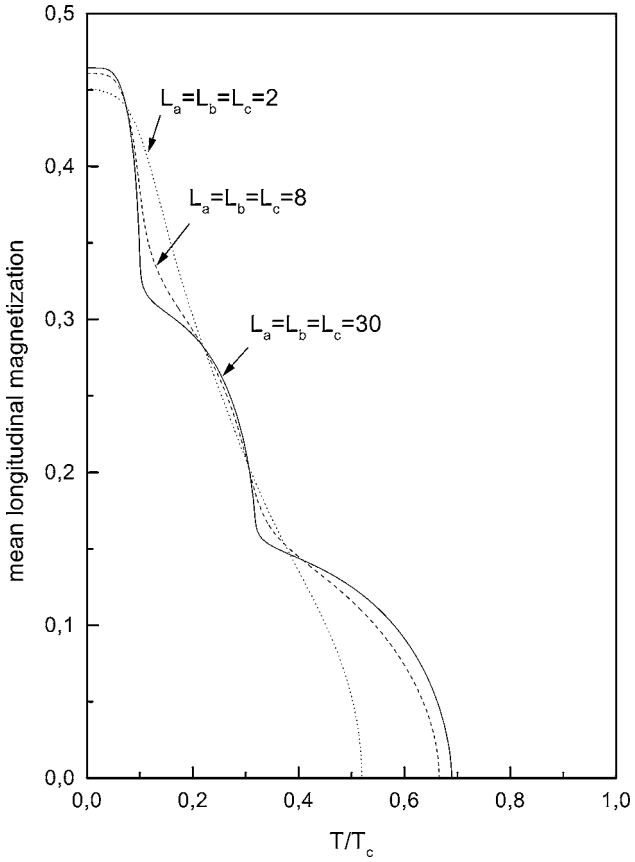

Fig. 7. The temperature dependence of the mean longitudinal polarization. Dashed for $A_2/B_2/C_2$ superlattice, dotted for $A_8/B_8/C_8$ superlattice, solid for $A_{30}/B_{30}/C_{30}$ superlattice.

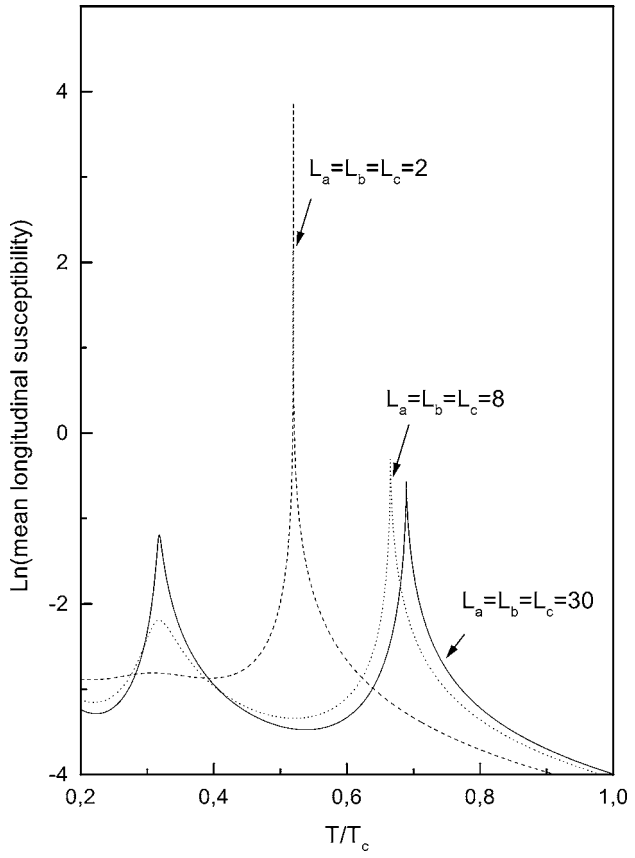

Fig. 8. The temperature dependence of the mean dieletric longitudinal susceptibility. Dashed for $A_2/B_2/C_2$ superlattice, dotted for $A_8/B_8/C_8$ superlattice, solid for $A_{30}/B_{30}/C_{30}$ superlattice.

position of the dielectric susceptibility shifts to longer periods. Similar results can be seen from Fig. 6b for temperatures above T_c^B, the period that shows a maximum dielectric susceptibility also tends to increase when the temperature approaches T_c. This feature implies that there is a size-driven phase transition in some layers of the superlattice. By recalling Figs. 3 and 4, the phase transition layers are the interface layers between the ferroelectric layers and the paraelectric layers.

Figs. 7 and 8 show the temperature dependences of the mean polarization and the mean dielectric susceptibility of superlattices with different periods. The polarization of $A_{30}/B_{30}/C_{30}$ superlattice decreases very quickly, but not to zero, at the value of T_c^B, so it is reasonable to define a ferroelectric-ferroelectric phase transition around T_c^B for $A_{30}/B_{30}/C_{30}$ superlattice in Fig. 7. As the period becomes smaller, see $A_8/B_8/C_8$ superlattice, the above feature becomes less obvious, but there is still a dielectric susceptibility peak around T_c^B. While in $A_2/B_2/C_2$ superlattice, no anomalies in polarization or dielectric susceptibility can be found around this temperature. This means that the behavior of the dielectric properties in the superlattice is mainly determined by the ferroelectric layers. The dielectric susceptibility peaks at T_c^B are mainly caused by the phase transition of B-layers in the superlattice. When the period is very small, the dielectric properties of B-layers is strongly influenced by the interface layers around it. If the period is small enough, the dielectric properties of the B-layers may differ essentially from that of the bulk material B. From Figs. 7 and 8, we can see that the Curie temperature of $A_{30}/B_{30}/C_{30}$ superlattice is higher than those of $A_8/B_8/C_8$ and $A_2/B_2/C_2$ superlattices, which is in agreement with our results shown in Fig. 2. However the transition temperature of the ferroelectric-ferroelectric phase transition is less affected by the period of the superlattice.

4. Conclusion

We have studied a three alternative layer ferroelectric superlattice $A_m/B_m/C_m$, where A-layers and B-layers are ferroelectric and C-layers are paraelectric. The Curie temperature is mainly determined by the thickness of the layers which have a higher Curie temperature, and it depends strongly upon the period of the superlattice when the period is small. The interface layers between the ferroelectric layers and paraelectric layers have strong influence on the properties of the superlattice. There is a polarization minimum and a dielectric susceptibility maximum around short period which shifts to longer period when the temperature approaches the phase transition temperature. When the period is large, there is a ferroelectric-ferroelectric phase transition below the Curie temperature. The results obtained are qualitatively similar to those obtained in [21]. The method used in this work is more exact than the mean field approximation, and the results are of great interest for both further theoretical work and experimental observations.

Acknowledgments

Two of the authors A. A. and M. S. gratefully acknowledge the hospitality of the Max Planck Institut für Physik Komplexer Systeme Dresden, Germany where this work has been initiated and the Picardie University, Amiens, France where it has been completed with the support of PROTATRS III D1208 and the Nato Support (Collaborative Linkage Grant project on "New Ferroelectric-Relaxor Oxydes for Microelectronic Applications") Reference: PST.CLG 980055.

Appendix I

Calculation of the layer dielectric longitudinal susceptibilities

By taking into account the applied longitudinal magnetic field h, the layer longitudinal polarizations take the form

$$m_{nz} = 2^{-N-2N_0}\sum_{\mu=0}^{N}\sum_{\mu_1=0}^{N_0}\sum_{\mu_2=0}^{N_0}\{C_\mu^N C_{\mu_1}^{N_0} C_{\mu_2}^{N_0}(1-2m_{nz})^{\mu} \times(1+2m_{nz})^{N-\mu}(1-2m_{n-1,z})^{\mu_1}(1+2m_{n-1,z})^{N_0-\mu_1} \times(1-2m_{n+1,z})^{\mu_2}(1+2m_{n+1,z})^{N_0-\mu_2}\times f_z(y_n+h,\Omega_n)\} \tag{A1}$$

with the periodic boundary conditions

$m_{nz}(n=0) = m_nz(n=L)$,

$m_{nz}(n=L+1) = m_{nz}(n=1)$,

$L = L_a + L_b + L_c + 3$

and where

$$y_n = \tfrac{1}{2}[J_{n,n}(N-2\mu) - J_{n,n-1}(N_0-2\mu_1) - J_{n,n+1}(N_0-2\mu_2)] \tag{A2}$$

and

$J^l_{1,0} \equiv J^l_{1,L} = J^l_{ac}$,

$J^l_{n,n-1} = J^l_{aa}$ for $2 \le n \le L_a$,

$J_{n,n} = J_{aa}$ for $1 \le n \le L_a$,

$J^l_{n,n+1} = J^l_{a,a}$ for $1 \le n \le L_a - 1$,

$J^l_{L_a,L_a+1} = J^l_{L_a+1,L_a} = J^l_{L_a+1,L_a+2} = J^l_{L_a+2,L_a+1} = J^l_{ab}$,

$J_{L_a+1,L_a+1} = J_{ab}$,

$J^l_{n,n-1} = J^l_{bb}$ for $L_a+3 \le n \le L_a+L_b+1$,

$J_{n,n} = J_{b,b}$ for $L_a+2 \le n \le L_a+L_b+1$,

$J^l_{n,n+1} = J^l_{bb}$ for $L_a+2 \le n \le L_a+L_b$,

$J^l_{L_a+L_b+1,L_a+L_b+2} = J^l_{L_a+L_b+2,L_a+L_b+1} = J^l_{L_a+L_b+2,L_a+L_b+3} = J^l_{L_a+L_b+3,L_a+L_b+2} = J^l_{bc}$,

$J_{L_a+L_b+2,L_a+L_b+2} = J_{bc}$,

$J^l_{n,n-1} = J^l_{cc}$ for $L_a+L_b+4 \le n \le L_a+L_b+L_c+2$,

$J_{n,n} = J_{cc}$ for $L_a+L_b+3 \le n \le L_a+L_b+L_c+2$,

$J^l_{n,n+1} = J^l_{cc}$ for $L_a+L_b+3 \le n \le L_a+L_b+L_c+1$,

$J^l_{L_a+L_b+L_c+2,L_a+L_b+L_c+3} = J^l_{L_a+L_b+L_c+3,L_a+L_b+L_c+2} = J^l_{L_a+L_b+L_c+3,L_a+L_b+L_c+4} = J^l_{L_a+L_b+L_c+4,L_a+L_b+L_c+3} = J^l_{ac}$,

$J_{L_a+L_b+L_c+3,L_a+L_b+L_c+3} = J_{ac}$,

$J^l_{L_a+L_b+L_c+4,L_a+L_b+L_c+3} \equiv J^l_{L+1,L} = J^l_{1,L} = J^l_{ac}$

and

$\Omega_n = \Omega_a$ for $1 \le n \le L_a$,

$\Omega_n = \Omega_{ab}$ for $n = L_a+1$,

$\Omega_n = \Omega_b$ for $L_a+2 \le n \le L_a+L_b+1$,

$\Omega_n = \Omega_{bc}$ for $n = L_a+L_b+2$,

$\Omega_n = \Omega_c$ for $L_a+L_b+3 \le n \le L_a+L_b+L_c+2$,

$\Omega_n = \Omega_{ac}$ for $n = L_a+L_b+L_c+3$.

By differentiating the equations of the layer longitudinal polarizations (Eqs. (A1)) with respect to h and taking the limit when h goes to zero, we get the following set of equations

$$\frac{\partial m_{nz}}{\partial h}\Big)_{h=0} = A^z_{n,n-1}\frac{\partial m_{n-1,z}}{\partial h}\Big)_{h=0} + A^z_{n,n}\frac{\partial m_{nz}}{\partial h}\Big)_{h=0} + A^z_{n,n+1}\frac{\partial m_{n+1,z}}{\partial h}\Big)_{h=0} + B^z_n. \tag{A3}$$

The set of Eqs. (A3) yields

$$C^z_{n,n-1}\chi_{n-1,z} + C^z_{n,n}\chi_{nz} + C^z_{n,n+1}\chi_{n+1,z} = 1 \quad \text{for } 1 \le n \le L \tag{A4}$$

with

$$C^z_{n,n-1} = -\frac{A^z_{n,n-1}}{B^z_n}, \qquad C^z_{n,n} = \frac{1-A^z_{n,n}}{B^z_n}, \qquad C^z_{n,n+1} = -\frac{A^z_{n,n+1}}{B^z_n}.$$

Eqs. (A4) are a set of L linear equations from which the layer dielectric longitudinal susceptibilities are obtained. The expressions of the coefficients appearing in the equations of the appendix are given by

$$A^z_{n,n-1} = 2^{-N-2N_0}\sum_{\mu=0}^{N}\sum_{\mu_1=0}^{N_0}\sum_{\mu_2=0}^{N_0}\sum_{i=0}^{\mu_1}\sum_{j=0}^{N_0-\mu_1}\{C_\mu^N C_{\mu_1}^{N_0} C_i^{\mu_1} C_j^{N_0-\mu_1} \times(-1)^i 2^{i+j}(i+j)(m_{n-1,z})^{i+j-1}(1-2m_{nz})^{\mu} \times(1+2m_{nz})^{N-\mu}(1-2m_{n+1,z})^{\mu_2}(1+2m_{n+1,z})^{N_0-\mu_2} \times f_z(y_n,\Omega_n)\}, \tag{A5}$$

$$A^z_{n,n} = 2^{-N-2N_0}\sum_{\mu=0}^{N}\sum_{\mu_1=0}^{N_0}\sum_{\mu_2=0}^{N_0}\sum_{i=0}^{\mu}\sum_{j=0}^{N-\mu}\{C_\mu^N C_{\mu_1}^{N_0} C_i^{\mu} C_j^{N-\mu} \times(-1)^i 2^{i+j}(i+j)(m_{nz})^{i+j-1}(1-2m_{n-1,z})^{\mu_1} \times(1+2m_{n-1,z})^{N_0-\mu_1}(1-2m_{n+1,z})^{\mu_2}(1+2m_{n+1,z})^{N_0-\mu_2} \times f_\alpha(y_n,\Omega_n)\}, \tag{A6}$$

$$A^z_{n,n+1} = 2^{-N-2N_0}\sum_{\mu=0}^{N}\sum_{\mu_1=0}^{N_0}\sum_{\mu_2=0}^{N_0}\sum_{i=0}^{\mu_1}\sum_{j=0}^{N_0-\mu_2}\{C_\mu^N C_{\mu_1}^{N_0} C_i^{\mu_2} C_j^{N_0-\mu 2} \times(-1)^i 2^{i+j}(i+j)(m_{n+1,z})^{i+j-1}(1-2m_{nz})^{\mu} \times(1+2m_{nz})^{N-\mu}(1-2m_{n-1,z})^{\mu_1}(1+2m_{n-1,z})^{N_0-\mu 1} \times f_\alpha(y_n,\Omega_n)\}, \tag{A7}$$

$$B^z_n = 2^{-N-2N_0}\sum_{\mu=0}^{N}\sum_{\mu_1=0}^{N_0}\sum_{\mu_2=0}^{N_0} C_\mu^N C_{\mu_1}^{N_0} C_{\mu_2}^{N_0}(1-2m_{nz})^{\mu} \times(1+2m_{nz})^{N-\mu}(1-2m_{n-1,z})^{\mu_1}(1+2m_{n-1,z})^{N_0-\mu_1} \times(1-2m_{n+1,z})^{\mu_2}(1+2m_{n+1,z})^{N_0-\mu_2} g_z(y_n,\Omega_n) \tag{A8}$$

where the function $g_z(y,\Omega)$ is given by

$$g_z(y,\Omega) = \frac{\partial f_z(y,\Omega)}{\partial h}\Big)_{h=0} = \frac{1}{2}\left\{\frac{\Omega^2}{(y^2+\Omega^2)^{\frac{3}{2}}}\tanh\left[\tfrac{1}{2}\beta(y^2+\Omega^2)^{\frac{1}{2}}\right] + \frac{\beta}{2}\frac{y^2}{(y^2+\Omega^2)} \times\{1-\tanh^2[\tfrac{1}{2}\beta(y^2+\Omega^2)^{\frac{1}{2}}]\}\right\}. \tag{A9}$$

References

1. Camley, R. E. and Barnes, J., Phys. Rev. Lett. **63**, 664 (1989).
2. Krebs, J. J., Lubitz, P., Chaiken, A. and Prinz, G. A., Phys. Rev. Lett. **63**, 1645 (1989).
3. Camley, R. E. and Tilley, D. R., Phys. Rev. B. **37**, 3413 (1988).
4. Iijima, K., Terashima, T., Bando, Y., Kamigaki, K. and Terauchi, H., Jpn. J. Appl. Phys. **72**, 2840 (1992).
5. O'Neill, D., Bowman, R. M. and Gregg, J. M., Appl. Phys. Lett. **77**, 1520 (2000).
6. Qu, B. D., Evstigneev, M., Johnson, D. J. and Prince, R. H., Appl. Phys. Lett. **72**, 1394 (1998).
7. Qu, B. D., Zhong, W. L. and Prince, R. H., Phys. Rev. B **55**, 11218 (1996).
8. Aouad, N. El., Laaboudi, B., Kerouad, M. and Saber, M., J. Phys: Condens Matter **13**, 797 (2001).
9. Ma, Y. Q., Xu, X. H. and Shen, J., Solid State Commun. **114**, 461 (2000).
10. Tilley, D. R., Solid State Commun. **65**, 657 (1988).
11. Schwenk, D., Fishman, F. and Schwabl, F., Phys. Rev. B **38**, 11618 (1988).
12. Schwenk, D., Fishman, F. and Schwabl, F., J. Phys: Condens. Matter **2**, 5409 (1990).
13. Schwenk, D., Fishman, F. and Schwabl, F., Ferroelectrics **104**, 349 (1990).
14. Qu, B. D., Zhong, W. L. and Zhang, P. L., Phys. Lett. A **189**, 419 (1994).
15. Qu, B. D., Zhong, W. L. and Zhang, P. L., Jpn. J. Appl. Phys. **34**, 4114 (1995).
16. Blink, R. and Zeks, B., "Soft Modes in Ferroelectrics Antiferroelectrics," (North-Holland, Amsterdam, 1974).
17. Wang, C. L. and Smith, S. R. P., J. Korean Phys. Soc. **32**, S382 (1998).
18. Sy, H. H., J. Phys: Condens. Matter **5**, 1213 (1993).
19. Saber, M., Ainane, A., Dujardin, F. and Stébé, B., Phys. Rev. B **59**, 6908 (1999).
20. Htoutou, K., Oubelkacem, A., Ainane, A. and Saber, M., Chin. J. Phys. **40**, 644 (2002).
21. Wang, C. L., Xin, Y., Wang, X. S., Zhong, W. L. and Zhang, P. L., Phys. Lett. A **268**, 117 (2000).
22. Ho Nyung Lee, Christen, H. M., Chisholm, M. F., Rouleau, C. M. and Lowndes, D. H., Nature **433**, 395 (2005).
23. Saber, M., Chin. J. Phys. **35**, 577 (1997).
24. Dujardin, F., Stébé, B., Ainane, A. and Saber, M., Physica A **269**, 322 (1999).
25. Ferchmin, A. R. and Maciejewski, W., J. Phys. C **12**, 4311 (1979).
26. Wang, C. L., Smith, S. R. P. and Tilley, D. R., J. Phys: Condens. Matter **6**, 9633 (1994).